

4

INJURY SCIENCE RESEARCH
Proceedings of the Twenty-Eighth International Workshop

Understanding and Minimizing Error in Cervical Spine Tensile Testing

V. C. Chancey, C. A. Van Ee, R. W. Nightingale,
D. L. Camacho, B. S. Myers

ABSTRACT

Cadaveric testing is a mainstay of injury characterization and the development of human tolerance corridors. In particular, cervical spine tolerance data are often obtained from segmental and whole cervical spine testing of cadaveric specimens. These specimens experimentally represent a compliant system that moves initially by rotation of the vertebrae, abruptly stiffens, and then fails at relatively low loads. As a consequence, attempts to estimate whole spine behavior from segmental test results can lead to significant errors. Moreover, efforts to model these experiments can yield surprisingly poor predictive ability. Careful examination of the stiffness associated with the mechanical coupling of the cadaver spine and test frame linkage friction may help explain and reduce these errors. For example, observations of the effects of linkage friction with the testing equipment and setup used in a tensile test study led to the inclusion of basic frictional effects in a developed computational model. The incorporation of friction improved the computational model's prediction by 70% throughout the loading range (0 N - 220 N). Similarly, accounting for coupling effects of the test specimen also reduced errors in predicted whole spine behavior by 50% during initial model development. The resulting computational model prediction was within the experimental response corridors. These data illustrate the need to fully characterize and describe the test frame and test methodology used to develop human biodynamic models.

INTRODUCTION

Data required to study cervical spine injury may be obtained through clinical observations and laboratory testing. Often, experimental testing requires not only an understanding of cervical spine biomechanics, but also an appreciation of the nuances associated with the mechanical apparatus and equipment used to create clinically observed injuries or biomechanical behavior in a laboratory setting. Cadaveric cervical spine testing can take many forms. Testing of a whole cadaver, a whole cervical spine with associated ligaments and soft tissue intact, a single motion segment, and individual anatomic components are all utilized to obtain properties and descriptions of behavior necessary for modeling.

Recently, the occurrence of cervical spine injuries resulting from air-bag deployment has lead researchers to hypotheses concerning the important contribution of tensile loading in the mechanism of these injuries. Occupant interaction with air bags can produce tensile neck loading that may result in serious and fatal neck injuries even for low velocity collisions (SCI, 1998; Maxeiner and Hahn, 1997; Blacksia, 1993; Perez, 1996; Kleinberger and Summers, 1997). As little tensile human tolerance data (Mertz and Patrick, 1967, 1971; Clemens and Burow, 1972; Cheng et al., 1982; Shea et al., 1992; Yoganandan et al., 1996) exists to describe the mechanisms and tolerance of injury of the human neck, developing guidelines and

evaluations of modifications in air-bag design or other additional injury prevention strategies remains challenging. Because several research efforts are currently underway to characterize tensile cervical spine behavior and investigate the mechanisms of tensile-related injuries (Van Ee et al., 2000, Yoganandan and Pintar, 1999; Ching, 1999), particular attention needs to be given to experimental test variables associated with tensile test protocols. During an ongoing tensile testing study (Van Ee et al., 2000, Van Ee et al., 1999) several observations were made in regard to mechanical behavior of the test setup, whole cervical spine testing, motion segment testing, and appropriate interpretations required for reasonable computational modeling.

While it is understood that nonideal mechanical behavior in the test device creates errors in test results, the extent of its importance in tensile neck testing has not been described. One such phenomenon associated with testing is friction. When a test apparatus allows motion in a particular degree of freedom, the resulting free motion is opposed by frictional effects. Low-friction materials, lubrication, and sliding or rolling bearings assist a designer in minimizing friction; however even low friction systems may significantly alter mechanical behavior. Testing, like tensile studies, that creates large normal forces on bearing surfaces may be prone to friction. Test frame stiffness, including mechanical coupling of the specimen, can also influence experimental measured structural properties. Therefore, the purpose of this paper is to examine the effects of system friction and test frame stiffness on predicted neck tensile behavior.

METHODS

Unembalmed male human cadaver specimens from the head through T2 were obtained. Medical records and pretest radiographs of the specimens were examined to ensure that there were not any unrecognized spinal pathologies that might degrade structural integrity. The mandible was removed to allow visualization of the upper cervical spine and allow for application of load to the maxilla. T1 and T2 were cleaned of muscular tissue and cast into an aluminum cup with reinforced polyester resin and polymethyl methacrylate (PMMA) allowing free motion at the C7-T1 level. Casting of T1-T2 was performed with the T1 vertebra oriented 25° down from the horizontal (-25° pitch) in the casting cup to preserve normal cervical lordosis (Matsushita et al., 1994). The skull was coupled to the head mount platform using bone screws and fiber reinforced acrylic. The head was cast so that the head mount frame was parallel to the Frankfurt plane. Care was taken to allow full motion at the Occiput-C1 level. An optical marker was placed on the specimen to approximate the head CG.

The head and neck were then placed in the experimental test frame (Figure 1). The test fixture applied a pure vertical load (based on the global coordinate system) at the center of the rotational bearing. Pure tensile loading was obtained by use of the linear and rotational bearings coupling the head to the hydraulic actuator. An RVDT located at a rotational bearing quantified head rotation. Two LVDTs were used to monitor the hydraulic actuator position and the linear bearing position. Either of the two cranial collected using a digital data acquisition system (National Instruments; Austin, TX).

Initial position for testing was established by positioning the head mount platform within the head carriage of the experimental frame so that the loading axis (bearing rod) was aligned through the approximate head CG and the Frankfurt plane was horizontal. The ram position was adjusted to achieve a compressive load of 22 N (the weight of the lower cast) resulting in a no load condition at the C7-T1 motion segment.

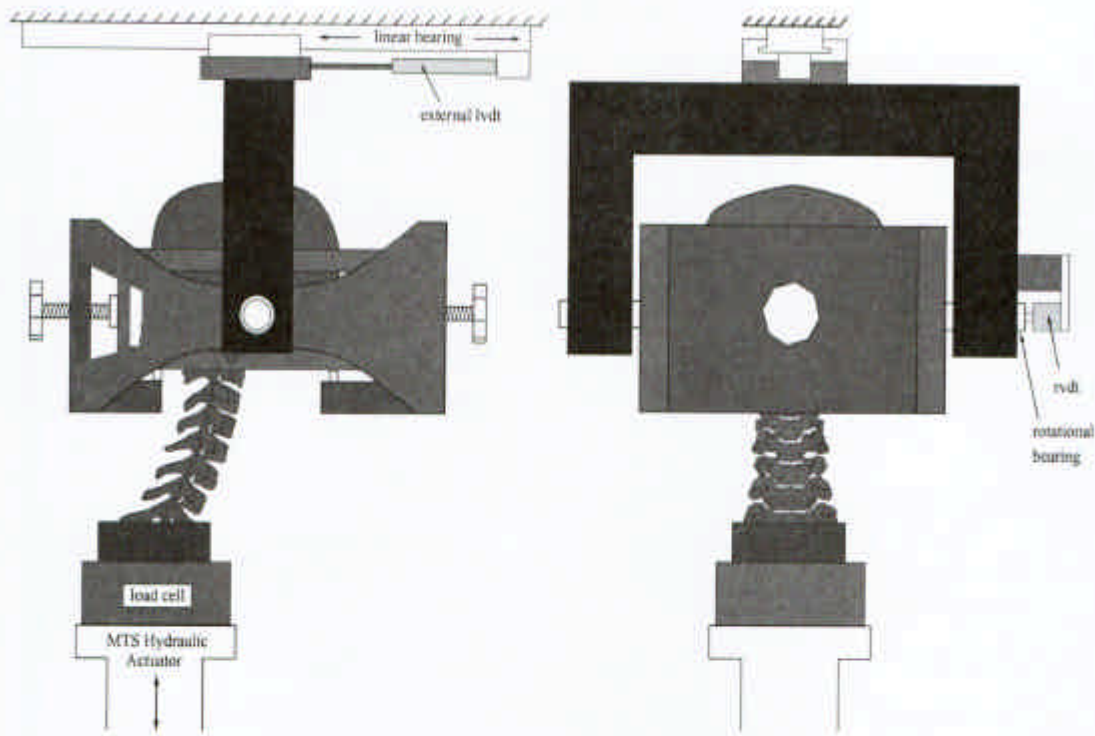


Figure 1. Test fixture used for tensile test experiments. The fixture produces a pure vertical load at the center of the rotational bearing by minimizing the shear and rotation through the use of the linear and rotational bearing respectively. Both the linear and rotational degrees of freedom can be fixed to apply varying end conditions.

The tests for each specimen are summarized in Table 1. Following the nondestructive whole cervical spine tests, the specimen was removed from the load frame and sectioned for motion segment testing. The spine was sectioned between C3-C4 and C5-C6 to give three intact and functional motion segments for testing, including the adjacent vertebral bodies, the intervertebral disc, posterior longitudinal ligament, ligamentum flavum, anterior longitudinal ligament, and intact articular facet capsules. The resulting segments, Occiput-C2, C4-C5, and C6-C7, were then cast individually to produce three motion segment test specimens. A single vertebra was cast using supra-pedicular loops traveling from the casting material through the vertebral foramen over the pedicle and back through the transverse foramen.

Corridors for the average response across specimens for each cranial end condition and line of action were defined by averaging the displacements and rotations across specimens at load steps of 20 N. The corridor response was defined as the average displacement \pm one standard deviation. Tensile displacement versus load responses were linearly regressed between 160 and 220 N. The slope was defined as flexibility and the y-intercept as the low-load displacement. Individual specimen motion segment stiffness tests were regressed using the exponential function

Table 1. Experimental Test Battery.

A. Non-Destructive Whole Cervical Spine Testing (Occiput-T1)			
Test	Description	Loading Location	End Condition
Fixed-Fixed Test	2 mm/s to peak load 300 N Record peak displacement, L_p	CG	Fixed
Mechanical Stabilization	30 cycles of 0.5 Hz sine wave with mean and amplitude of 25% L_p	CG	Fixed
Stiffness Test	2 mm/s to peak load 300 N	CG	Fixed
End Condition Tests	2 mm/s to peak load 200 N	CG	Free Rotational Constraint Translational Constraint
Line of Action Test	2 mm/s to peak load 200N	CG 3 cm anterior CG Condyles 3 cm post- Condyles	Fixed

B. Non-Destructive Motion Segment Testing (Occiput-C2, C4-C5, C6-C7)			
Test	Description	Loading Location	End Condition
Motion Segment Setup	Occiput-C2 C4-C5, C6-C7	CG	Load placed to produce small extension (3 deg)
Fixed-Fixed Test	2 mm/s to peak load 300 N Record peak displacement, L_p	CG	Fixed
Mechanical Stabilization	30 cycles of 0.5 Hz sine wave with mean and amplitude of 25% L_p	CG	Fixed
Stiffness Test	2 mm/s to peak load 300 N	CG	Fixed

$$F_z = A(e^{kz} - 1) \tag{1}$$

The average tensile displacement versus load response from the fixed-fixed whole cervical spine tests and the fixed-fixed motion segment tests were compared. A simple lumped parameter whole cervical spine representation was formed from a combination of motion segment springs. The summed motion segment responses were used to investigate the effects of frame stiffness, initial offsets, and low-load behavior outside the more complex finite element rigid body representation developed for the tensile ligamentous model.

The cervical spine model presented by Camacho et al. (1997) that was validated for compression impacts was used as a foundation for the tensile ligamentous model. The model consists of rigid body vertebra and a finite element head coupled together by Kelvin solids (a parallel spring and damper). In the sagittal plane, two translational Kelvin solids and one rotational Kelvin solid couple the superior vertebra to the next inferior vertebra (Figure 2). The joint kinetics are defined about the center of rotation (COR). The COR is located at a node connected to the superior body and defined as the midpoint of the CG's of the adjacent vertebral bodies. The translational Kelvin solids are connected to the COR and external nodes of the inferior body which are 10 cm from the COR in the X or Z direction. Linear damping constants and nonlinear spring properties were determined by pure moment flexion-extension experiments and data available in the literature (Camacho et al., 1997).

The tensile properties of the joint models were revised based on the fixed-fixed whole ligamentous spine stiffness test and the average motion segment stiffness response. The fixed-fixed whole ligamentous

spine test was used for model construction. Individual motion segment tensile response curve shape was defined based on the average motion segment stiffness response of the ligamentous spine tests and linearly extrapolated beyond load levels of 360 N.

A series of pulleys and weights were used to measure the friction of the linear translation slide with roller bearing that supports the head carriage and allows free translation of the upper fixation during end condition testing. Similarly, the force to overcome friction in the rotational bearing with rolling surface contact was measured. The location and use of the bearings within the test apparatus are shown in Figure 1.

To simulate the experimental test apparatus, the friction of the translational and rotational bearings was modeled using an elastic-plastic spring. The translational spring had an elastic stiffness of 10,000 N/m, yield load of 3.5 N, and a tangent stiffness of 1 N/m. The rotational spring had an elastic stiffness of 1 Nm/deg, yield load of 0.75 Nm, and a tangent stiffness of 1.7×10^{-5} Nm/deg.

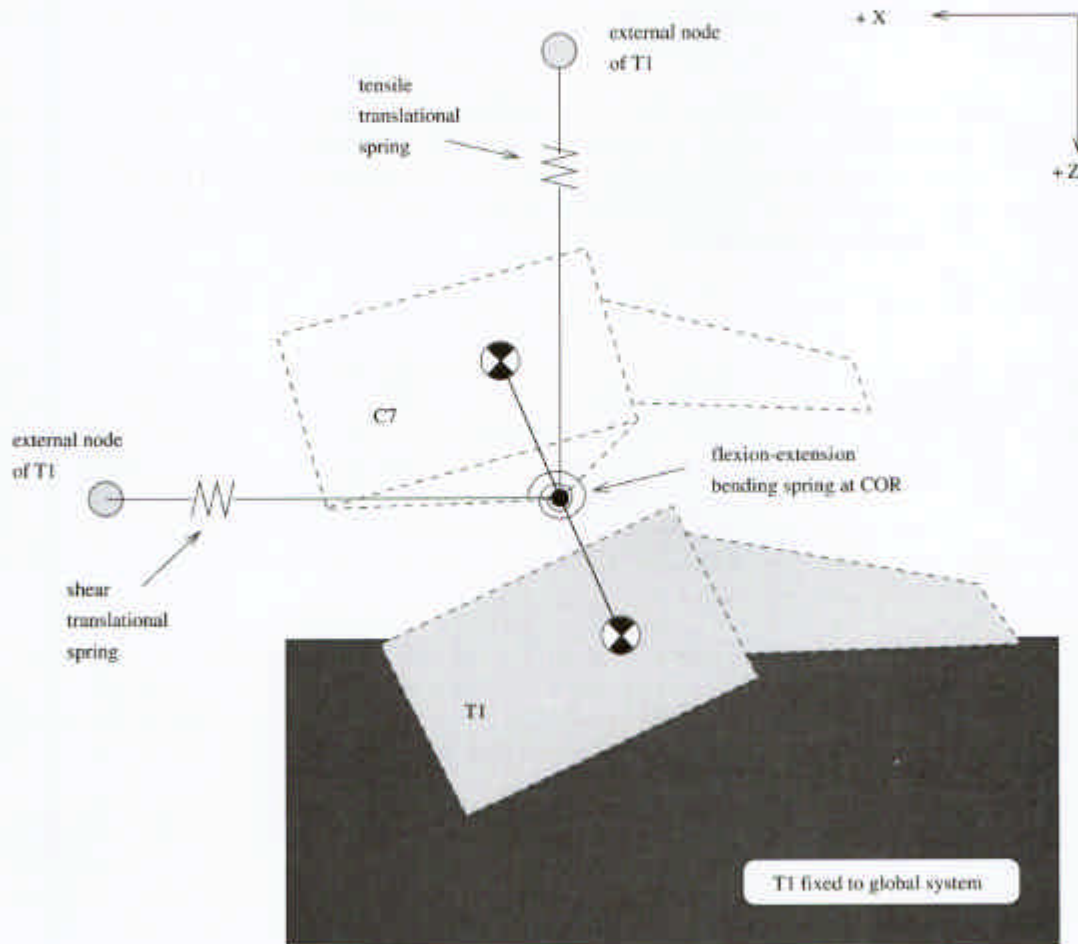


Figure 2. Schematic of the model of sagittal plane motion applied to the motion segment of C7-T1.

The response of the ligamentous model was validated by comparing the predicted displacement response with the experimental response for free, rotationally constrained, and the translationally constrained end

conditions. In addition, the model was validated against the line of action tests. Comparisons of ram displacement, carriage translation, and carriage rotation were made at tensile load steps of 20 N. RMS error for validation and error source quantification was computed for each response using

$$RMS_{error} = \sqrt{\frac{\sum (\bar{Y}_{exp} - Y_{model})^2}{n}} \quad (2)$$

where \bar{Y}_{exp} was the experimental mean and Y_{model} was the model prediction.

RESULTS

Head and neck tensile response was greatly influenced by the cranial end condition exhibiting both decreases in stiffness of 60% and increases in the low-load elongation of 1000% as the end conditions changed from fixed to free. Stiffness for the fixed, rotational, translational and free end conditions were 69, 56, 42 and 27 N/mm respectively, and low-load elongations were 1.1, 1.1, 6.5, and 10.5 mm respectively.

Motion segment stiffness was found to have only a moderate low load region. The average correlation coefficient for the exponential fits of individual specimen stiffness response was 0.995 ± 0.002 . No significant differences were found in the motion segment stiffness response at any of the 20 N load levels (Figure 3). The motion segment stiffness properties were combined yielding an average motion segment stiffness response function (Equation 3).

$$F_z = 320(e^{0.396\Delta z} - 1) \quad (3)$$

Using this response, the simple representation of the whole cervical spine as a series of the motion segments is less stiff than the experimentally observed whole cervical spine (Figure 4). Over the loading region of 160 – 220 N, the average motion segment stiffness is 204 N/mm. Summing seven of these average motion segment stiffnesses in series creates a whole cervical spine stiffness of 29 N/mm, which is 57% less stiff than the observed experimental whole cervical spine response (69 N/mm) over the same load range. Comparing the simple series model response to the average experimental whole cervical spine response, the RMS error difference is 2.54 mm, three times the standard deviation of the experimental whole cervical spine response.

By considering the effects of a measured frame stiffness of 900 N/mm placed in series with each test specimen, motion segment and whole cervical spine, reduces RMS error by 34%. This adjustment is not enough to match the simple spring model response to the experimental average whole cervical spine response (Figure 5). A 300 N/mm spring in series with each motion segment eliminates 97% of the error.

Small constant deflections due to specimen coupling or frame compliance does not change the shape of the measured response however it can reduce error (Figure 6). When an offset of 0.1 mm in each motion segment is removed from the motion segment response, there is an overall 19% improvement in the simple model. An experimentally unmeasurable slip of 0.05 mm between the specimen and fixation material at each fixation end can give rise to a 0.1 mm offset in each test, and thereby significant error.

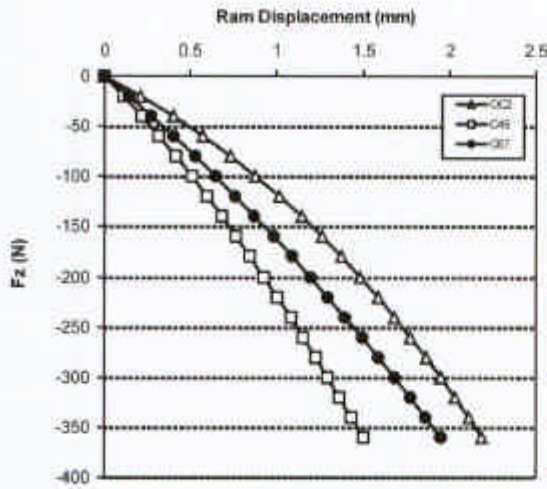


Figure 3. Average stiffness response of O-C2, C4-C5, and C6-C7.

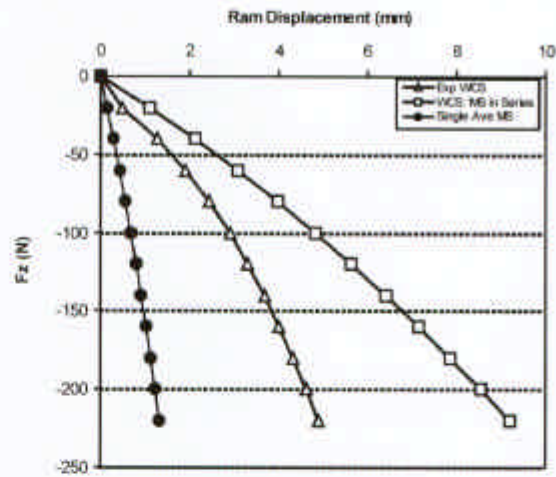


Figure 4. Relative stiffness characteristics of a simple lumped parameter spring model.

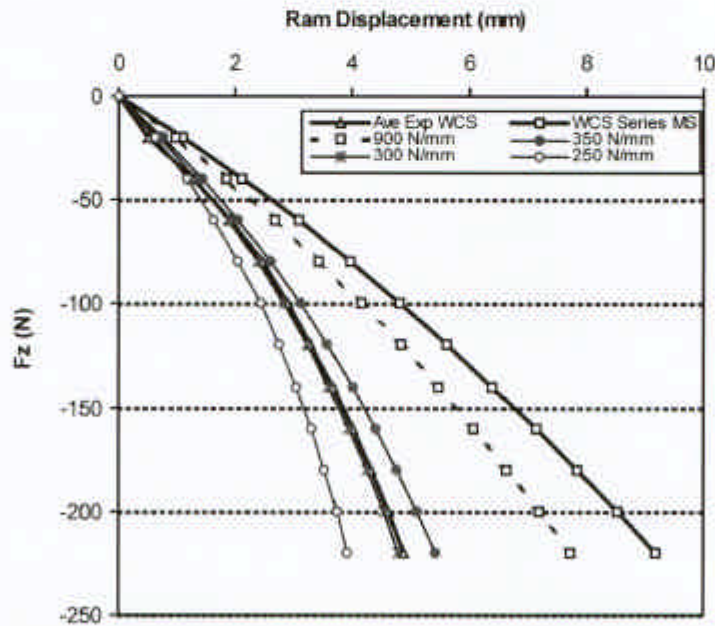


Figure 5. A snapshot of the influence of several series stiffness contributions, like frame stiffness, on the force deflection behavior of the simple series model.

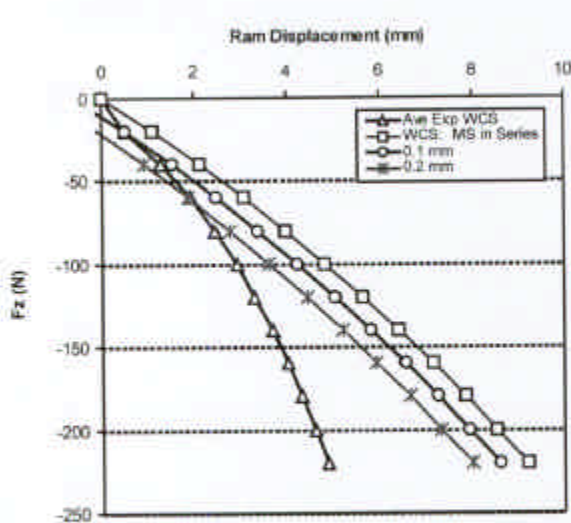


Figure 6. Initial position effects measured error.

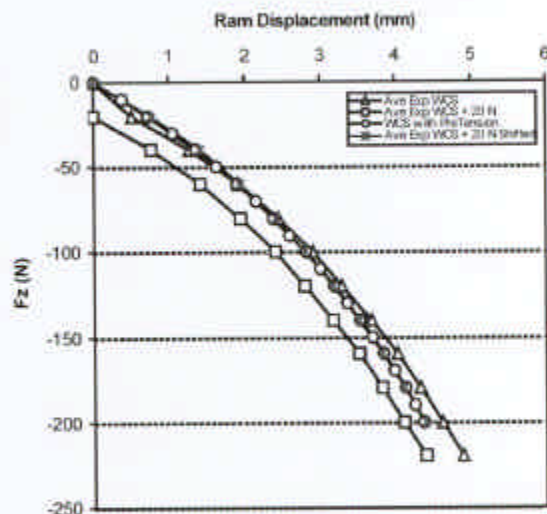


Figure 7. Illustration of the difference of removal of 20 N of compressive preload causes in the whole cervical spine response in a fixed-fixed test.

The removal of a pre-test compressive load results in no change in stiffness behavior (within a standard deviation) and reduces the region of low load behavior. Indeed, less than 2% difference in stiffness in the upper load range is observed. However, when the series model is adjusted for the removal 20 N of pre-compression and compared to the pre-tension response, the difference is 25% less than the difference shown in Figure 4. A single whole cervical spine response without pre-compression is less than 5% different from the shifted average whole cervical spine response. Together, frame stiffness, low load behavior due to preload, and small slippage displacements account for only 55% of the error observed in a simple series model.

Modeling the friction of the translational and rotational bearings in the experimental apparatus was found to significantly improve the low load predicted response and accuracy of the finite element rigid body ligamentous spine model. In the free end condition, modeling the effect of friction decreased the RMS error by 68%, 75%, and 74% for ram displacement, carriage translation, and carriage rotation respectively (Figure 8).

Neglecting the frictional forces led to errors in the low load (20-60 N) predictive ability of the model on the order of 900% - 2000%. Modeling the effect of friction also resulted in a slip-stick phenomenon that was also observed experimentally. The results of the slip-stick phenomenon resulted in discontinuities in the slope of the response, particularly visible in the low-load region.

Model predictions of the tensile force displacement response for the cranial end conditions of free, rotation constrained and translation constrained were consistent with the experimental corridors (Figure 9). The model was found to predict the end condition responses with an average RMS error of 0.82 mm, 4.9 mm, and 2.3 deg which is 8%, 43%, and 11% of the full scale values for ram displacement, carriage translation, and carriage rotation, respectively. The corresponding average standard deviation across

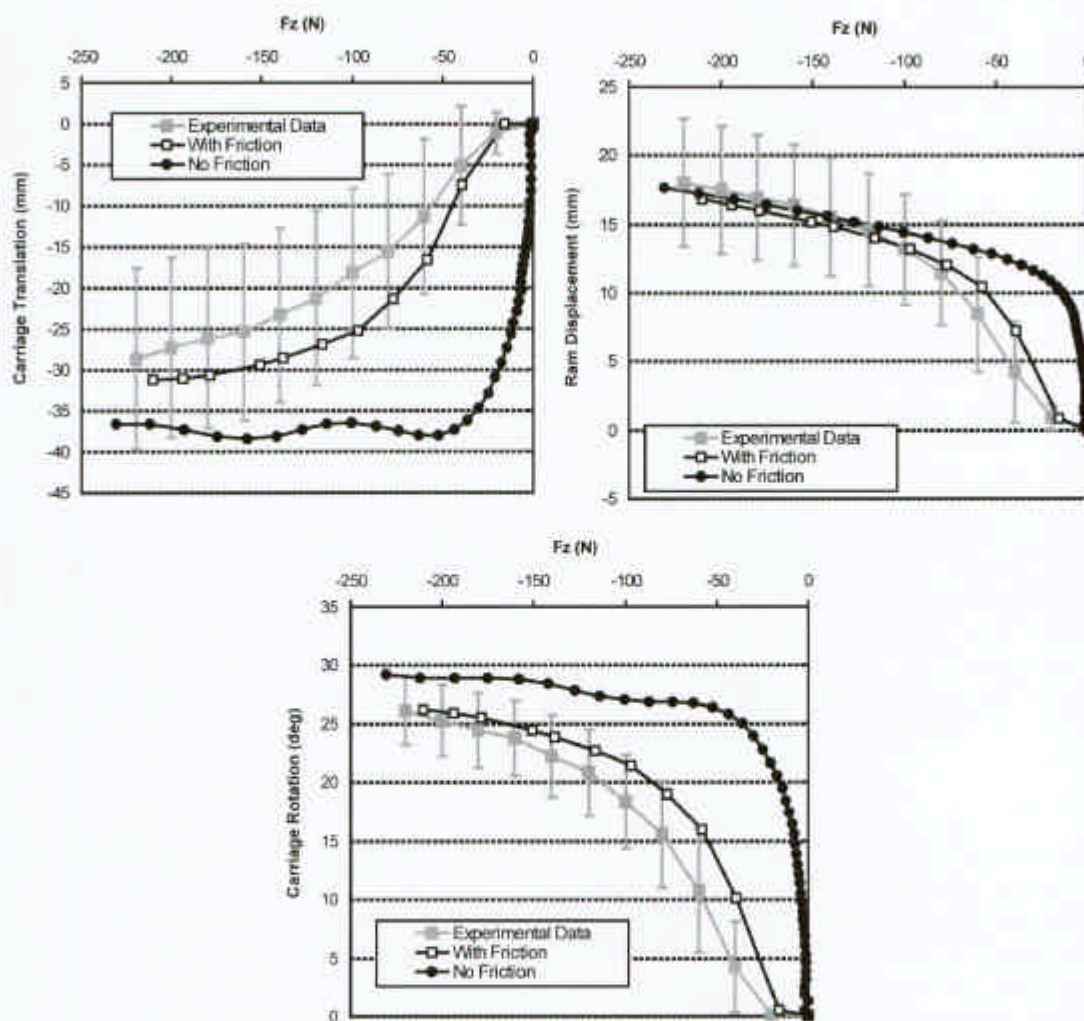


Figure 8. The effect of friction on model performance for the free end condition is evident particularly in the low load region.

specimens for these responses was 1.80 mm, 7.4 mm, and 2.3 deg for ram displacement, carriage translation, and carriage rotation, respectively. In that respect the model prediction was well within the experimental corridor when properly accounting for the frame stiffness, no load region, and friction.

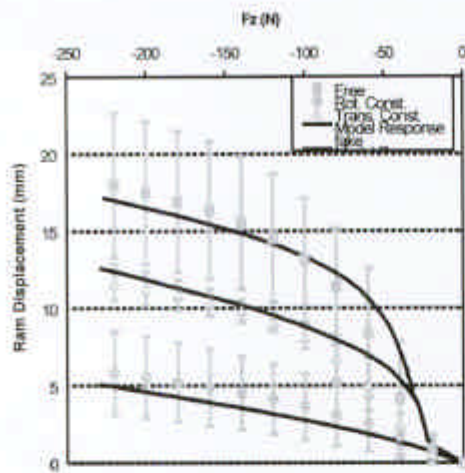


Figure 9. The model predicted the response due to cranial end condition within the experimental data corridors defined by one standard deviation.

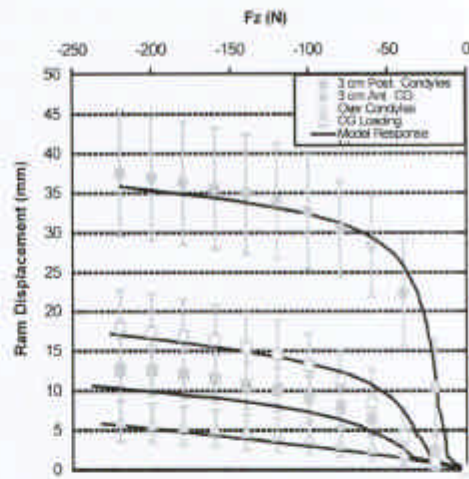


Figure 10. The model predicted the response due to tensile load eccentricity within the experimental data corridors defined by one standard deviation.

Similarly the model predictions for the effect of anteroposterior eccentricity of the tensile load, as quantified by the line of action tests, were consistently within the experimental corridors (Figure 10). The model was found to predict the line of action tests with an average RMS error of 1.4 mm, 6.2 mm, and 2.4 deg which is 10%, 36%, and 103% of the full scale for ram displacement, carriage translation, and carriage rotation, respectively (Figure 8). The corresponding average standard deviation across specimens for these responses was 3.6 mm, 6.9 mm, and 2.4 deg for ram displacement, carriage translation, and carriage rotation, respectively.

DISCUSSION

Motion segment tensile stiffnesses exhibited a wide range with average linear stiffness properties for lower cervical segments of 212 ± 96 N/mm and a secant stiffness at 300 N of 253 ± 65 N/mm. Liu et al. (1982) reported greater linear stiffness properties of 381 ± 136 N/mm for lower cervical motion segments. An analysis of the results of Liu et al. supported the finding of this study that no significant differences in stiffness were found between spinal levels. Shea et al. (1991) reported cervical stiffness to range from 157 to 433 N/mm and also did not find cervical level to significantly affect tensile stiffness. White and Panjabi (1990) reported a much lower cervical motion segment stiffness of 53 N/mm. The relatively wide range of motion segment stiffness properties, 53 - 433 N/mm, reported likely reflect errors in frame compliance, grip slip, no load region, and the experimental response.

Considering frame compliance in this study was not sufficient to completely resolve the difference between a simple whole cervical spine model composed of motion segments in series (Figure 5) and the experimental response. The measured frame compliance produced significant difference (34%) in overall measured stiffness response. The addition of a 300 N/mm series stiffness reduced the difference between the response built from series motion segment tensile responses and the average whole cervical spine by 97%. Such a low stiffness (observed motion segment stiffness was 204 N/mm) in the mechanical system external to the specimen is unlikely however and was not present in the current test frame or methodology. Accordingly, other factors not directly related to the test frame need to be investigated to

quantify their effects. Small error may result from the pull-out of k-wires and bone screws from PMMA (Flahiff, Gober, and Nicholas, 1995), PMMA and fiber reinforced acrylic interaction, the strength and bending properties of k-wires and pedicle loops, and the application of the loading through the k-wires and pedicle loops onto the vertebral bone.

A simple lumped parameter spring model (Figure 4 – 6) suggests additional biomechanical phenomena influence the whole cervical spine model built from motion segment data. The process of sectioning the spine into motion segments disrupts ligamentous fibers, including the longitudinal and supraspinous ligaments, that span several motion segments. Adams (1995) suggests this procedure, although extremely useful, may lead to an underestimation of the contribution of ligament tensile strength.

An additional source of variation in behavior may result from loading through the low load or neutral zone of a specimen. Each tested specimen has potential anatomical and fixation backlash, similar to backlash in mechanical gear systems, as the specimen undergoes compressive loading, no load, and then experiences tensile loading. During these conditions, the application of compressive preloads to achieve a no load state at C7-T1 could allow small displacement error. The number of segments required to build the whole cervical spine model amplifies this distance and the resulting behavior. The 0.5 mm change (10% of full scale displacement in the fixed-fixed stiffness tests) associated with 20 N of axial force is only 0.2 mm less than that projected in a simple model based on seven motion segment responses if each had a 0.1 mm offset. The replacement of compression with small tensile preload only slightly changes the higher load stiffness behavior (less than 2%) but effectively shifts load-displacement behavior (Figure 6). The use of tensile preload in specimen testing for tensile behavior is similar to common manufacturing practice for the use of extension springs.

The importance of accurately modeling the experimental conditions was also evident with the effect of friction on model predictions. While the frictional loads were less than 1.5% of the full scale tensile loads, the effect on model kinetics was large and needs to be accounted for in the model.

CONCLUSIONS

Data collected through the use of a uniform tensile test methodology was used in the development and validation of computational models of the cervical spine. While the series arrangement of spinal motion segments into a whole spine model appears to be a simple task, significant errors were produced. Consideration of the non-ideal features of the test frame including friction, test frame stiffness, and no-load initial position significantly reduce by half, but do not eliminate, these errors. As such whole spine testing is still required to design and validate whole spine models. By using the structural responses of the whole spine and the motion segments with experimental environment factors, a computational ligamentous spine model was developed which was free of these errors and successfully validated against a variety of tensile loading conditions. The model predicted the mean experimental response with an average RMS error less than the average standard deviation across specimens.

ACKNOWLEDGEMENTS

This study was supported by the National Highway Traffic Safety Administration cooperative agreement DTNH22-94-Y-07133.

REFERENCES

- ADAMS, M.A. (1995). Spine update: Mechanical testing of the spine. *Spine*, **20**, 2151-2156.
- BLACKSIN, M.F., (1993). Patterns of fracture after air bag deployment. *J. Trauma*, **35**, 840-843.

- BYARS, E.F., HAYNES, D., DURHAM, T., and LILLY, H., (1970). Craniometric Measurements of Human Skulls. ASME Publication 70-WA/BHF-8, 1-11.
- CHENG, R., YANG, K., LEVINE, R., KING, A., and MORGAN, R., (1982). Injuries to the cervical spine caused by a distributed frontal load to the chest. Proc. 26th Stapp Car Crash Conference, SAE Paper No. 821155.
- CLEMENS, H.J. and BUROW, K., (1972). Experimental investigation on injury mechanism of cervical spine at frontal and rear-front vehicle impacts. Proc. of the 16th Stapp Car Crash Conference, SAE Paper No. 720960.
- CHING, R., (1999). Personal Communication.
- FLAHIFF, C.M., GOBER, G.A., and NICHOLAS, R.W., (1995). Pullout strength of fixation screws from polymethylmethacrylate bone cement. *Biomaterials*, **16**, 533-536.
- KLEINBERGER, M. and SUMMERS, L., (1997). Mechanisms of injuries for adults and children resulting from airbag interaction. Proc. 41st Association for the Advancement of Automotive Medicine.
- MATSUSHITA, T., SATO, T. B., HIRABAYASHI, K., FUJIMURA, S., ASAZUMA, T., and TAKATORI, T., (1994). X-Ray Study of the Human Neck Motion Due to Head Inertia Loading. Proc. 38rd Stapp Car Crash Conference, SAE Paper No. 942208, 55-64.
- MAXEINER, H. and HAHN, M., (1997). Airbag-induced lethal cervical trauma. *J Trauma*, **42**, 1148-1151.
- MCCELHANEY, J.H., HOPPER, R.H., NIGHTINGALE, R.W., and MYERS, B.S., (1995). Mechanisms of Basilar Skull Fracture. *Journal of Neurotrauma*, **12**, 669-678.
- MERTZ, H.J. and PATRICK, L.M., (1967). Investigation of the Kinematics and Kinetics of Whiplash. Proc. 11th Stapp Car Crash Conference, SAE Paper No. 670919.
- MERTZ, H.J., and PATRICK, L.M., (1971). Strength and Response of the Human Neck. Proc. 15th Stapp Car Crash Conference, SAE Paper No. 710855.
- MYKLEBUST, J.B., PINTAR, F., YOGANANDAN, N., CUSICK, J., MAIMAN, D., MYERS, T.J., and SANCES, A., (1988). Tensile strength of spinal ligaments. *Spine*, **13**, 526-531.
- SCI, (1998). Special Crash Investigation Program - Air Bag Investigations, National Highway Traffic Safety Administration, Washington, DC.
- SHEA, M., WITTENBERG, R.H., EDWARDS, W.T., WHITE, A.A. III, and HAYES, W.C., (1992). In vitro hyperextension injuries in the human cadaveric cervical spine. *J. Orthop. Res.*, **10**, 911-916.
- SHEA, M., EDWARDS, W.T., WHITE, A.A., and HAYES, W.C., (1991). Variations of stiffness and strength along the human cervical spine. *J. Biomechanics*, **24**, 95-107.
- VAN EE, C. A., CHASSE, A. L., and MYERS, B. S., (2000). Quantifying Skeletal Muscle Properties in Cadaveric Test Specimens: Effects of Mechanical Loading, Postmortem Time, and Freezer Storage. *J. Biomechanical Engineering*, **122**, 9-14.

WHITE, A.A. and PANJABI, M.M. (1990). *Clinical biomechanics of the Spine*. J.B. Lippincott Company, Philadelphia.

YOGANANDAN, N., PINTAR, F.A., MAIMAN, D.J., CUSICK, J.F., SANCES, A., JR., and WALSH, P.R., (1996). Human Head-Neck Biomechanics under Axial Tension. *Med. Eng. Phys.* **18**, 289-294.

YOGANANDAN, N., PINTAR, F.A., (1999). Personal Communication.

